



Technical Note

Effect of turbulence on Taylor dispersion for oscillatory flows

Xiaofeng Ye^{*}, Jiangwu Zhang*Institute of Mechanical Engineering, Shanghai Jiaotong University, Shanghai 200030, China*

Received 22 January 2002

Abstract

Experiments were carried out to explore the effect of the turbulence on Taylor dispersion for oscillatory tube flow. We found from measured velocity profiles that, while the velocity fluctuations exist over the parameter range in the present investigation, periodic conditional turbulent flow occurs and the turbulence intensity increases rapidly when the Stokes layer-based Reynolds number exceeds 535. The effective axial mass diffusivity for oscillatory flow deviate from the theoretical predictions corresponding to laminar flow as Re_δ value increases, and the deviation becomes noticeable as Re_δ increases to 235. It was also found that an ratio of effective diffusivity to theoretical value for laminar flow as large as 100 is available during turbulent oscillatory flows. © 2002 Elsevier Science Ltd. All rights reserved.

1. Introduction

Over the past several decades, mass and heat dispersion enhancement for time-periodic flows has assumed great importance in the fields of medical and chemical industrial engineering. Harris and Goren [1] investigated the mass dispersion characteristics of chemical solute through a long tube connecting two reservoirs of different concentration during pulsed flow and found that the axial transfer rate of HCl in water can be increases from 10- to 60-fold over that due to molecular diffusion alone. Joshi et al. [2] made experiments on gas exchange augmentation in straight tubes, with the results demonstrating that, under the condition of oscillatory flows, the concentration of O₂ gas spreads longitudinally at rates orders of magnitude greater than the value of molecular diffusion coefficient of O₂. This enhanced dispersion leads to a typical successful practical application of oscillatory flow—high frequency ventilation (HFV). Due to the similarity between the mass diffusion and heat conduction equations, an equivalent enhanced process should occur in the heat-transfer area. In fact, by replacing Schmidt number with Prandtl number, the two problems become nearly identical with the only exception being the difference in the wall

boundary conditions. Kurzweg [3] confirmed the existence of such an enhanced heat-transfer process in oscillatory flows within a capillary bundle connecting two reservoirs maintained at different temperatures. Using water as the working fluid, effective thermal diffusivities some four orders of magnitude larger than the thermal diffusivity value for water were measured. The corresponding heat-transfer rates are comparable to those achievable with heat pipes and thus suggest that the phenomena may find important applications in areas requiring rapid heat removal.

Mass transport in straight tube is governed by Taylor-type dispersion [4,5], which is called augmented dispersion because of its enhancement effect on axial spread of diffusing substance. The virtual longitudinal diffusion transport during oscillatory flow arises due to the axial convection in conjunction with radial molecular diffusion. In fact, the radial diffusion is essential for axial dispersion, i.e., it is the lack of perfect reversibility of tracer concentration profile that causes particles to migrate to different locations at each oscillation cycle.

Theoretical investigations of dispersion for laminar oscillatory flows in straight tubes have been made by Chatwin [6] and Watson [7]. Their theories have demonstrated that, under the condition of oscillatory flows, the effective dispersion in axial direction is governed by the interaction of the radially dependent axial-velocity profile and the corresponding radially varying concentration

^{*} Corresponding author.

Nomenclature

C	concentration	Re_δ	Reynolds number based on Stokes layer thickness, $Re/\alpha\sqrt{2}$
d	tube diameter	Sc	Schmidt number, ν/D_{mol}
D_{eff}	effective diffusivity	t	time
D_{mol}	molecular diffusivity	$u(r, t)$	axial velocity
$(D_{\text{eff}})_{\text{lami}}$	D_{eff} for laminar flow	$\langle u(r, t) \rangle$	ensemble-average velocity, cf. Eq. (3)
$(D_{\text{eff}})_{\text{turb}}$	D_{eff} for turbulent flow	$u'(r, t)$	turbulent velocity
f	oscillation frequency	\bar{u}	root-mean-square averaged velocity
$f(\alpha, Sc)$	function, cf. Eq. (5)	Δx	tidal displacement
$I(r)$	turbulent intensity	z	distance
M	amount of tracer	<i>Greek symbols</i>	
N	number of oscillation cycles	α	Womersley number, $R\sqrt{(\omega/\nu)}$
Pe	Peclet number, $2R\bar{u}/D_{\text{mol}}$	η	dimensionless radial coordinate
Q	flow rate	ν	kinematic viscosity
r	radial coordinate	ω	angular frequency
Re	Reynolds number, $2R\bar{u}/\nu$		

profile and found that the maximum value of effective diffusivity corresponds to the condition that the radial diffusion time scale is comparable to half the oscillation period. The predictions by their theories are consistent with the experiments by Joshi et al. [2], and Kurzweg [3,8].

The interest in mass transport has arisen regarding the effects of turbulent flow on Taylor dispersion. Lee [9] performed experiments to visualize the mixing and axial spread of smoke in turbulent oscillatory flows, and Kamm et al. [10] investigated the effect of turbulent jet (superposed on oscillatory flow having a small net flow) on axial dispersion. Their experiments have show that, as the Reynolds number increases, the velocity fluctuations and turbulence of flow affect the radial mixing considerably. Nevertheless, few papers, either theoretical or experimental, have been published on longitudinal diffusion for turbulent oscillatory flows, in comparison

with the large number of investigations on that for laminar flows.

2. Experimental arrangement

The present work was conducted in a lucite pipe having inner diameter of 6 mm and length of 300 cm. The pipe was connected through bell mouths to a reservoir at one end and, at the other end, to a piston chamber (i.d. 150 mm) inside which a fender plate in combination with the smoothed inner surface of bell mouth plays a role of buffering and straightening flows. The schematic arrangement of the apparatus is shown in Fig. 1.

The oscillation of fluid inside the test tube was generated by a piston driven by a DC motor through a Scotch-yoke mechanism, thus the cross-sectional mean flow rate in the axial direction varied sinusoidally.

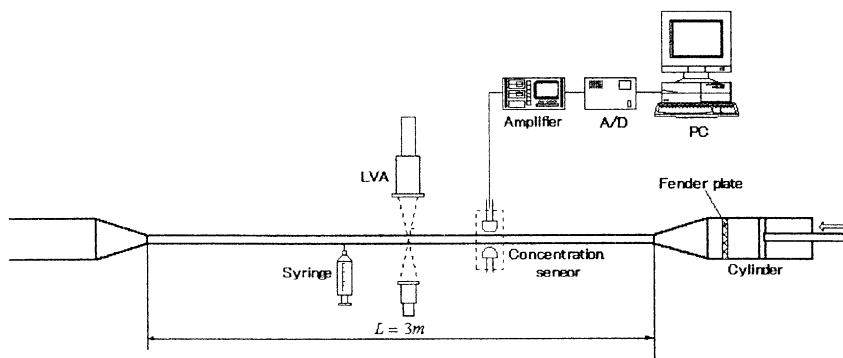


Fig. 1. Experimental arrangement.

In the present experiments, the stroke volume could be varied over the range 0.66–32 cm³ and the frequency of oscillation was adjustable from 0–3 Hz, with Reynolds number ranged from 185 to 13,000 and Womersley number, α , ranged from 3.52 to 10.87, so as the flow regime stretching over the transition Re value in the stability diagram established by Hino et al. [11] for oscillatory flows. The working fluid used in the experiment was city water.

3. Turbulence in oscillatory tube flow

3.1. Velocity measurement

Measurements of axial velocity component of oscillatory flow were performed using a Laser-Doppler Anemometer, LDA (Model DISA 55×, DISA electronic Co., Ltd., Denmark). The LDA used here to work in one-component forward-scatter mode. A certain amount of milk was mixed into the working fluid as seeding particles, which are required by the LDA measurement method. The LDA signals were processed in a counter-type processor. The particle arrival rate was sufficiently high (always larger than 1000 s⁻¹) for the signals to be regarded as continuous.

Measurements were made near the midpoint of the test tube with distance between the measurement point and the tube ends long adequately (>200 i.d.), thus there should be no influence of the entrance effect in velocity data.

3.2. Velocity profiles and variations for oscillatory flows

The range of the flow parameters used in velocity measurements was consistent with that used in the investigations of diffusivity characteristics. Experiments were first conducted for oscillatory flows at relatively small oscillation amplitude of fluid and low Stokes layer-based Reynolds number. Fig. 2 shows the typical profiles of velocity distribution obtained at different radial positions for $\Delta x/d = 19$ and $Re_\delta = 160$. These curves were obtained not simultaneously but independently. The result of Fourier analysis shows that at this small value of Δx and Re_δ , the variations of the axial velocity are smooth, which indicates the flow being in laminar regime. Though the axial velocities in Fig. 2 vary sinusoidally with time, the velocities in the core region have a slight phase delay with respect to those near the wall, leading to annular velocity profiles. Fig. 3 is constructed to illustrate clearly the variations of this phase lag with the inflexion points existing near the wall.

Though the curves in Fig. 3 are smooth and of sinusoidal on the whole, there is a little noise on the velocity signal recorded at the central position of the tube. This means the slight deviation of the velocity from the theoretical one for laminar flow. Measurements show

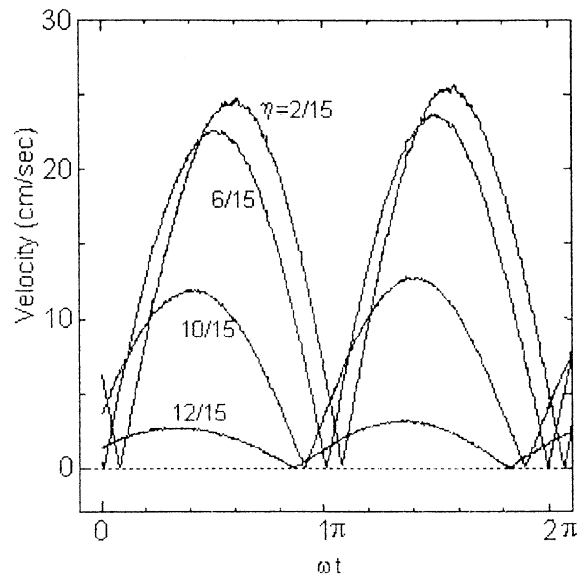


Fig. 2. Temporal velocity variation at different radial positions for $\Delta x/d = 19$ and $Re_\delta = 160$.

that, with the Stokes layer-based Reynolds number Re_δ below 105, the flow remains fairly laminar and, as Re_δ increases to about 340, the distortion of the velocity from laminar becomes evident.

As the tidal displacement Δx and Re_δ were increased further, it was observed from the velocity records that noticeable turbulent bursts occurred near the wall during certain periods of the cycle. Fig. 4 shows a typical temporal axial velocity variations at the tube centerline and near the wall at the onset of turbulence for $\Delta x/d = 75$ and $Re_\delta = 632$. It is noted from this figure that the velocity fluctuations near the wall are much stronger than in the centerline of the tube. This implies that the instabilities were generated near the wall and the radial momentum transfer caused a lower level of velocity fluctuations near the centerline. This is because, at high Reynolds numbers, the annular effect becomes pronounced and there exist inflexion points in the velocity profile near the wall. Thus, at a critical value of the Stokes layer Reynolds number, the fluid flow near the wall may first become unstable and eddies occur near the wall. These eddies, transferred to the core flow, causes small fluctuations. We found that turbulence disappeared and the flow recovered to a laminar-like flow in the accelerating period of the half cycle for which a favorable pressure gradient exists.

Fig. 5, in which ensemble-average velocities $\langle u(r, t) \rangle$ (hollow triangle mark) are plotted on the same abscissa, is used to compare these with the theoretical laminar oscillatory flow (dot lines). In the decelerating stage, the velocity at the central position decreases suddenly,

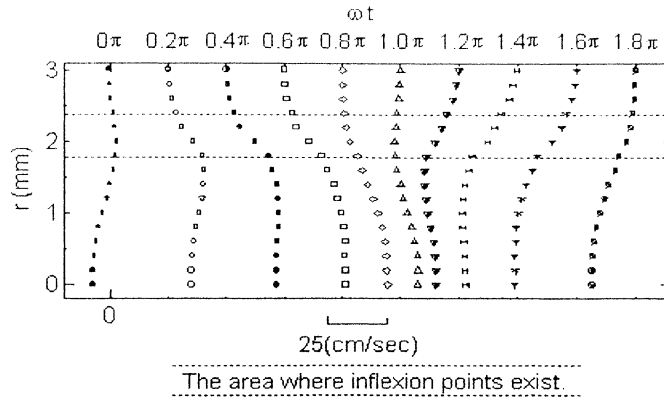


Fig. 3. Velocity profiles at different moments. $\Delta x/d = 38$ and $Re_\delta = 320$.

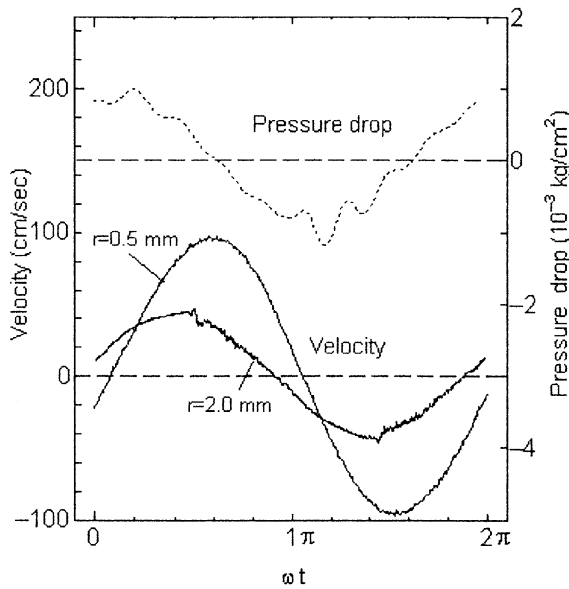


Fig. 4. Temporal variations of the pressure gradient and the axial velocity near the tube wall. $\Delta x/d = 75$ and $Re_\delta = 632$.

accompanied by violent turbulent fluctuations, while near the wall, the velocity increases rapidly above the laminar value confirming the generation of large-scale eddies across the tube section.

3.3. Turbulence intensity of oscillatory flows

In steady flows, when the Reynolds number exceeds a certain value, the velocity of fluid fluctuates about its mean value in a random manner. The same holds for oscillatory flow (Fig. 6).

The velocity fluctuation is defined as

$$u'_i(r, t) = u_i(r, t) - \langle u(r, t) \rangle \quad (1)$$

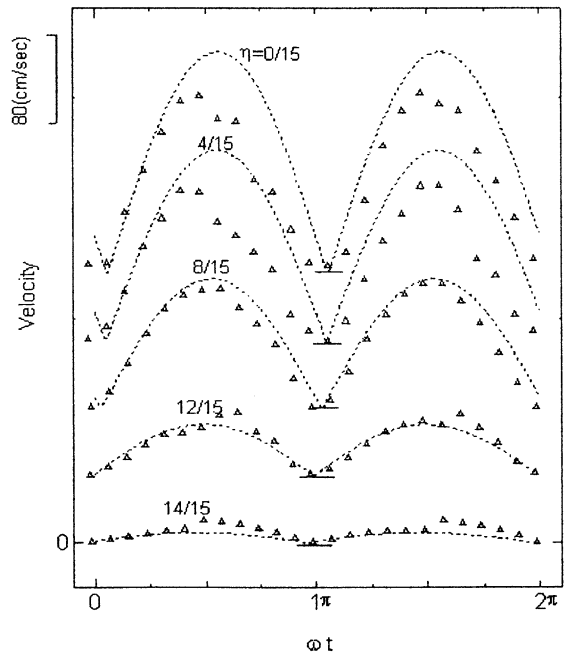


Fig. 5. Measured velocity variations compared with the theoretical predictions for laminar flow. $\Delta x/d = 97$ and $Re_\delta = 815$.

where $\langle u(r, t) \rangle$ is the ensemble-averaged velocity and obtained by the segmented velocity data for each cycle $u_i(r, t)$ ($i = 1, 2, \dots, N$), i.e.

$$\langle u(r, t) \rangle = \frac{1}{N} \sum_{i=1}^N u_i(r, t) \quad (2)$$

where N is the number of cycles sampled. The turbulence intensity is calculated

$$I(r) = \sqrt{\langle u'_i(r, t)^2 \rangle} \quad (3)$$

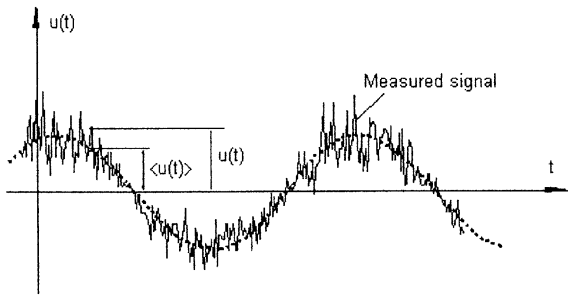


Fig. 6. An example of velocity fluctuation for turbulent oscillatory flow.

The measurements of velocity were executed at the radial location of $r = (1/4)d$, the calculated values of turbulence intensity are shown in Fig. 7. It may be seen that, the tendency of the turbulence intensity for four oscillation frequencies can be represented by a single curve, indicating the strong dependence of Re_δ on turbulence intensity. Although obviously the increasing of turbulence intensity becomes fast when Re_δ exceeds about 540 turbulent fluctuation exists undoubtedly over the whole flow parameter range in the present investigation. The increasing of turbulence intensity is steep for $540 < Re_\delta < 850$, whereas the increasing of momentum

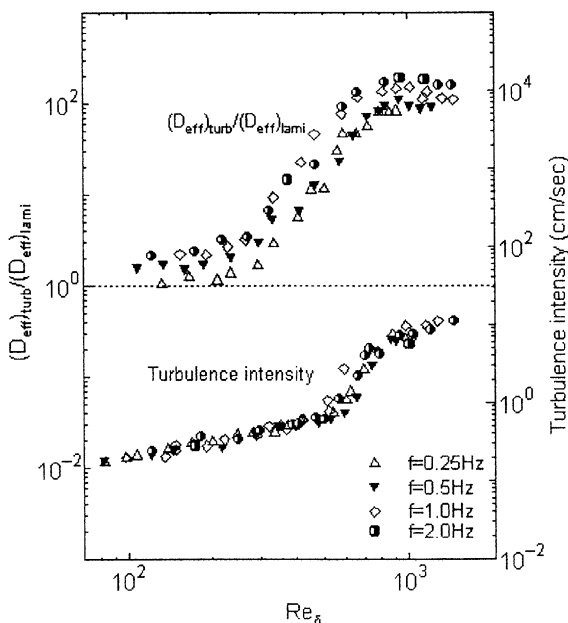


Fig. 7. Upper part: Ratio of experimentally measured effective diffusivity to that of the corresponding theoretical predictions for laminar flow. Lower part: Turbulence intensity of oscillatory flow measured at radial position of $r = (1/4)d$.

becomes weak when Re_δ exceeds about 1000 probably due to limitation of the tube cross-section which restrains the bursting and diffusion of large turbulent eddies.

The instability of oscillatory flows has been analyzed theoretically by Conrad and Crimalle [12], von Kerczek and Davis [13,14]. The energy theories of Davis and von Kerczek [15] give a relatively low critical Reynolds number sufficient for stability (Re_δ about 40–50 for two-dimensional disturbances), while the full theory of von Kerczek and Davis [13] predicts absolute stability within the investigated range ($Re_\delta < 800$).

Experiments on oscillatory flow instability have been carried out by Li [16] for the Stokes layer on smooth and by Sergeev [17] for oscillatory flow. The critical Stokes-layer Reynolds number has been determined, respectively, to be $Re_\delta = 565$ for the Stokes layer on a smooth wall and $Re_\delta = 500$ for oscillatory pipe flow. Hino et al. [11] investigated the transition to turbulence in oscillatory pipe flow, the critical Reynolds number $Re_\delta \cong 550$ applies satisfactorily for transition to conditional turbulence in nearly all the oscillatory flows.

The above-mentioned theoretical and experimental results of critical Reynolds number are scattered significantly. In fact, the experiments, except for those performed under rigorous control conditions, are susceptible to finite amplitude disturbances, which generally reduces the critical value. The discrepancies may be attributable partly to different transition criteria employed. In most experiments hitherto reported (e.g. [16]), the instability limit was determined by visual observation of tracer dye, while in the present work direct measurements of velocity variation were carried out.

4. Characteristics of longitudinal diffusion

4.1. Concentration measurement

To evaluate the characteristics of mass diffusion in the axial direction, a soluble dye of molecular diffusion coefficient of $2.78 \times 10^{-5} \text{ cm}^2/\text{s}$ was used as tracer. The small diffusivity of this tracer is suitable for the present purpose of revealing the influence of flow turbulence on Taylor dispersion.

A bolus of tracer (0.2 ml) was syringe-injected into the test tube at about mid-length with its injection phase being accurately controlled. The tracer concentration in the test tube was determined by measuring the intensity decrement of the light beam (from a light emitting diode) directed along the tube diameter perpendicular to the tube axis. The light detector at the opposite side of the tube was a photodiode with the peak-sensitive wavelength of 560 nm (Model BS500B, SHARP Co., Ltd., Japan).

4.2. Determination of effective diffusivity

The effective diffusivity was determined using the pulse-injection method employed in previous related investigations [18–20]. In order to obtain a pulse-like initial concentration distribution of tracer, injections were executed by a computer-operated system. The timing of injection was adjustable with respect to the oscillation phase of fluid. Injection at oscillation phase of 270° is recommendable because it was the very moment when the fluid was at rest (more exactly, the mean fluid flux over the cross-section of tube is zero) with the maximum displacement, the effect of the disturbance caused by injection on the flow inside the tube is considered to be negligible.

Since the internal diameter of the test tube was as small as 6.0 mm with the test tube being as long as 3.0 m, the axial diffusion of tracer can be assumed to be in one-dimensional manner. Under this assumption, the cross-sectional average concentration of tracer at position z (the distance from the injection point) after time t can be expressed as

$$C(z, t) = \frac{M}{2\sqrt{\pi D_{\text{eff}} t}} e^{-z^2/4D_{\text{eff}} t} \quad (4)$$

where D_{eff} is the effective diffusivity.

The effective diffusivities were determined by fitting Eq. (4) to the measured concentration values at the injection phase.

5. Effect of turbulence on longitudinal diffusion

The upper part of Fig. 7 shows, as a function of Reynolds number, the ratio of experimentally measured effective diffusivity to that of the corresponding theoretical predictions for laminar flow based on the analytical investigation of Watson [7]. It is seen from Fig. 7 that, for the lowest frequency used (0.25 Hz) and small tidal displacement, which means low Reynolds number, the values of $(D_{\text{eff}})_{\text{turb}}/(D_{\text{eff}})_{\text{lami}}$ are near 1.0. This implies that, for small Stokes-layer Re , the flow is in laminar regime and the radial mixing arises mainly due to the molecular diffusion.

Since the tracer employed is of small molecular diffusivity, the axial dispersion is sensitive to the velocity fluctuations and the influence of fluctuations of flow begins to appear relatively early as the flow parameters increase. When Re_δ exceeds 235, all the points for $(D_{\text{eff}})_{\text{turb}}/(D_{\text{eff}})_{\text{lami}}$ deviate from the value of 1.0. But in the region of $Re_\delta = 105\text{--}235$, it is clear that the increase rate of $(D_{\text{eff}})_{\text{turb}}/(D_{\text{eff}})_{\text{lami}}$ is smaller than that of turbulence intensity. This is because that the flow in this Re_δ range is in the regime of distorted laminar flow yet, the fluctuations of the flow velocity are in a low level.

In fact, not only the strength of velocity fluctuations or turbulence but also the phase at which the velocity fluctuations present affects the axial dispersion. Physically speaking, the mechanism of the augmented longitudinal dispersion is that the axial fluid motion sows throughout its journey the particles, which are migrating radially owing to molecular diffusion or turbulence, the lack of the reversibility of concentration profile for each oscillation cycle causes the particles to locate at different positions resulting in an augmented axial dispersion. Hence, it would be naturally followed that, radial migration at too early phase of oscillation (i.e. small fluid displacement) is not desirable and, though hard to expect to occur in practical situation, radial mixing occurring explosively at the moment when displacement of fluid is maximum will be the most ideal circumstance to augment the longitudinal dispersion. For Re_δ in the range of 105–235, the flow is of distorted laminar and the velocity fluctuations present near the peak on the flow velocity curve, which corresponds to about half the displacement amplitude. This interprets to a certain extent that the velocity fluctuations for the Re_δ value smaller than 235 augment the axial dispersion not so significantly.

As Reynolds number increases further, the axial dispersion is strongly augmented with the deviations of D_{eff} from theoretical values becoming noticeable. When the Stokes-layer Re exceeds about 580, flow becomes conditionally turbulent, in which violent turbulence with high frequency is generated in the decelerating period and the turbulence disappears suddenly in the reversed accelerating period. Since the enhanced lateral turbulent mixing occurs during the period when the displacement of fluid is beyond half its amplitude, the longitudinal dispersion is thus augmented greatly. In Fig. 7, the large values of $(D_{\text{eff}})_{\text{turb}}/(D_{\text{eff}})_{\text{lami}}$ indicate that the dispersion process is dominated by the turbulence for the oscillatory flow in conditionally turbulence regime.

In previous studies [7] on the mass dispersion in laminar oscillatory flows, it has been shown that, the effective dispersion in axial direction is produced by the interaction of the radially dependent axial-velocity profile and the corresponding radially varying concentration profile and can be described by

$$D_{\text{eff}} = D_{\text{mol}}(1 + f(\alpha, Sc)Pe^2) \quad (5)$$

where the first term in the right-hand side is responsible for the contribution of molecular diffusion of tracer and usually negligible for diffusion process in liquid fluid, and the second term accounts for the interaction of axial convection with radial diffusion.

Eq. (5) shows that, through an appropriate normalization, all the diffusion processes for a given Schmidt number can be represented by a single curve. Among the various factors used to normalize Eq. (5), $\Delta x^2 \omega$ has been

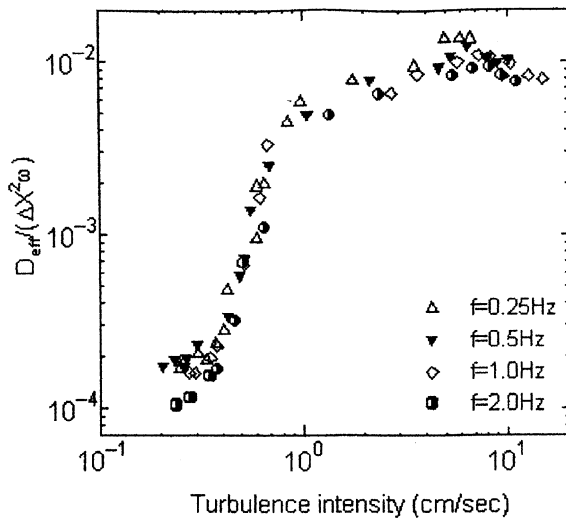


Fig. 8. Correlation of longitudinal diffusivity to turbulence intensity.

used extensively because of its rationality that, for the diffusion during oscillatory flow both the concentration gradient in radial direction and the area of the contacting surface of boundary layer with flow core are proportional to the tidal displacement, and ω is a measure of the number of oscillation cycles per unit time. The data normalized by $\Delta x^2 \omega$ is a measure of the efficiency of the system used enhance the longitudinal dispersion process.

Fig. 8 shows a correlation of the normalized value of longitudinal diffusivity to turbulence intensity. The plot indicate that, for weak turbulent flows the normalized dispersion coefficients rise fast as the turbulent intensity increases, while the turbulent intensity exceeds a certain value, the values fall. According to the theoretical analysis by Kurzweg [3], for laminar oscillatory viscous flows, the effective mass diffusivity reaches a maximum when the radial diffusion time scale is comparable to half the oscillation period. Though we have not got the expression to calculate the radial mixing time scale for conditionally turbulent flows, it can be deduced with rationality that, the peak of the normalized effective diffusivity in Fig. 8 corresponds to the very circumstance that the equivalent lateral mixing time scale is equal to half the oscillation period.

6. Conclusions

The velocity profile and variation of oscillatory tube flow have been measured. It was noted that the axial velocities in the core-flow region have phase delays with respect to those near the tube wall. These delays lead to

annular velocity profiles on which inflexion points exist near the wall.

The velocity records showed that, when the Stokes layer-based Re increases to a certain value, turbulent fluctuations occur during certain times of the oscillation cycle and the turbulent fluctuations near the tube wall are much stronger than in the centerline of the tube.

The experiments on turbulence showed that, the increasing of turbulence intensity becomes fast when Re_δ exceeds about 535, which is slightly smaller than that proposed by previous investigators as the critical value for transition to turbulent flow. It was found also that the change from a favorable pressure gradient to a reversed pressure gradient is responsible for the onset of turbulence.

As Re_δ increases, the measured values for effective diffusivities deviate from the corresponding theoretical predictions for laminar flow and the deviation becomes noticeable when Re_δ increases to 235. This implies that the dispersion process is influenced and gradually dominated by turbulence as Re_δ increases. It is seen from Fig. 8 that, the data points have peak at the turbulence of about 6 cm/s.

References

- [1] H.G. Harris, S.L. Goren, Axial dispersion in a cylinder with pulsed flow, *Chem. Eng. Sci.* 22 (1967) 1571–1576.
- [2] C.H. Joshi, R.D. Kamm, J.M. Dragen, A.S. Slutsky, An experiment study of gas exchange in laminar oscillatory flow, *J. Fluid Mech.* 133 (1983) 245–254.
- [3] U.H. Kurzweg, Enhanced heat conduction in oscillating viscous flows within parallel-plate channel, *J. Fluid Mech.* 156 (1985) 291–300.
- [4] G.I. Taylor, Dispersion of soluble matter in solvent flowing slowly through a tube, *Proc. R. Soc. London Ser. A* 219 (1953) 186–203.
- [5] G.I. Taylor, The dispersion of matter in turbulent flow through a pipe, *Proc. R. Soc. London Ser. A* 223 (1954) 446–468.
- [6] P.C. Chatwin, On the longitudinal dispersion of passive contaminant in oscillatory flows in tubes, *J. Fluid Mech.* 71 (1975) 512–527.
- [7] E.J. Watson, Diffusion in oscillatory pipe flow, *J. Fluid Mech.* 133 (1983) 233–244.
- [8] U.H. Kurzweg, G. Howell, Enhanced dispersion in oscillatory flows, *Phys. Fluids* 27 (1984) 1046–1048.
- [9] J.S. Lee, The mixing and axial transport of smoke in oscillatory tube flows, *Ann. Biomed. Eng.* 12 (1984) 371–383.
- [10] R.D. Kamm, E.T. Bullister, C. Keramidis, The effect of a turbulent jet on gas transport during oscillatory flow, *ASME J. Biomech. Eng.* 108 (1986) 266–272.
- [11] M. Hino, M. Sawamoto, S. Takasu, Experiments on transition to turbulence in an oscillatory pipe flow, *J. Fluid Mech.* 75 (1976) 193–207.

- [12] P.W. Conrad, W.O. Crimiale, *Z. Angew Math. Phys.* 16 (1965) 233.
- [13] C. von Kerczek, S.H. Davis, The stability of oscillatory Stokes layers, *J. Fluid Mech.* 51 (1972) 239–252.
- [14] C. von Kerczek, S.H. Davis, Linear stability of oscillatory Stokes layers, *J. Fluid Mech.* 62 (1974) 753–773.
- [15] S.H. Davis, C. von Kerczek, A reformulation of energy stability theory, *Arch. Rat. Meth. Anal.* 52 (1973) 112–117.
- [16] H. Li, Stability of oscillatory laminar flow along a wall, Beach Erosion Bd, Corps Engrs, USA, Tech. Memo. 47 (1954).
- [17] S.I. Sergeev, Fluid oscillations in pipes at moderate Reynolds numbers, *Fluid Dyn. (Mekh. Zh.)* 1 (1966) 21–22.
- [18] D. Elad, D. Halpern, J.B. Grotberg, Gas dispersion in volume-cycled tube flow. I. Theory, *J. Appl. Physiol.* 72 (1992) 312–320.
- [19] D.P. Gaver III, J. Solway, N. Punjabi, D. Elad, J.B. Grotberg, N. Gavriely, Gas dispersion in volume-cycled tube flow II. Tracer bolus experiments, *J. Appl. Physiol.* 72 (1992) 321–331.
- [20] Y. Xiaofeng, M. Shimizu, Longitudinal transport and frictional losses of grooved tubes for oscillatory flow, *J. Energy Heat Mass transfer* 21 (1999) 127–137.